Fitting MAS NMR spectra in crystals with local disorder: Czjzek's vs. Maurer's model for 11 B and 71 Ga in polycrystalline gallium borate

K. Seleznyova, N.A. Sergeev, M. Olszewski, P. Stępień, S.V. Yagupov, M.B. Strugatsky, J. Kliava

Fitting MAS NMR spectra in crystals with local disorder: Czjzek's vs. Maurer's model for ^{11}B and ^{71}Ga in polycrystalline gallium borate

K. Seleznyova[a,b], N.A. Sergeev[c], M. Olszewski[c], P. Stępień[c], S.V. Yagupov[b], M.B. Strugatsky[b], J. Kliava[a,*]

[a] *LOMA, UMR 5798 Université de Bordeaux-CNRS, 33405 Talence cedex, France*
[b] *Physics and Technology Institute, Crimean Federal V.I. Vernadsky University, 295-007 Simferopol, Republic of Crimea*
[c] *Institute of Physics, University of Szczecin, 15 Wielkopolska Str., 70-451 Szczecin, Poland*

A B S T R A C T

A comparative analysis of the Czjzek's and Maurer's models of the joint distribution density of NMR quadrupole parameters has been carried out in view of their application to account for spectra broadening induced by local disorder in crystals. As an example of such an application, we have considered Magic Angle Spinning NMR of ^{11}B and ^{71}Ga isotopes in polycrystalline gallium borate. Computer simulations carried out using both models unambiguously show that in the case of low local disorder the Maurer's model, in contrast to the Czjzek's model, provides satisfactory fits to experimental NMR spectra.

1. Introduction

Extracting meaningful physical information from Nuclear Magnetic Resonance (NMR) spectra requires accurate computer simulations. Fitting to experimental NMR spectra usually allows estimating chemical shifts and quadrupole parameters [1,2]. However, the existence of disorder in the environment of magnetic (with nuclear spin $I \neq 0$), in particular, quadrupolar ($I > \frac{1}{2}$) nuclei manifests itself in broadening of the spectra. As a consequence, relative amplitudes and widths of spectra features can be satisfactorily fitted to only if local disorder is explicitly taken into account in the simulation code, allowing for *statistical distributions* of the NMR parameters, in particular of the quadrupole parameters related to components of the electric field gradient (EFG) tensor.

From the viewpoint of the magnetic resonance (both electronic and nuclear) spectroscopist, different degrees of local disorder give rise to more or less broad distributions of relevant spectroscopic parameters. Therefore, in most cases, the degree of disorder can be defined with respect to the ratio distribution width/mean value of the most representative parameters. Typically, low local disorder occurs in high quality crystals possessing low concentrations of structure defects [3] while high local disorder is observed in non crystalline, in particular glassy solids [4] as well as in crystals with highly flawed structure [5,6]. In what follows, we shall refer to low and high degree of disorder in accordance with the above mentioned criterion.

The issue of the distribution of the quadrupole parameters was first raised by Czjzek in the framework of a random packing model of amorphous materials [7,8]. As far as the quadrupole parameters are related to components of the EFG tensor, Czjzek *et al.* suggested a joint distribution density (JDD) of these parameters. Later, Le Caër and Brand [9] have provided a more general justification of the Czjzek's JDD; indeed, they have shown that it holds if all components of the EFG (in NMR) or of the quadrupole fine structure (in Electron Paramagnetic Resonance, EPR) tensor are subjected to normal (Gaussian) random distributions. The Czjzek's JDD has been extensively used in both NMR and EPR studies of non crystalline materials [10–12] and also applied to simulate NMR spectra of some crystals with high degree of local disorder [5]. Yet, the major drawback of this JDD is to completely disregard symmetry and local structure persisting to a certain extent in crystals with low degree of disorder.

With the aim to describe a randomly distorted structure preserving, to a certain extent, local ordering, a more elaborated JDD of the quadrupole parameters has been suggested by Maurer [13] and Le Caër and Brand [9]. For brevity, we refer to this JDD as the Maurer's model, although Le Caër and Brand have provided a more detailed theoretical analysis thereof. Interestingly, a similar model has been put forward to describe the JDD of nanoparticle size and shape distribution [14].

The aim of the present work is to evaluate the applicability of the Czjzek's and Maurer's JDDs to NMR studies of only slightly disordered crystals. As an example, we have treated the NMR Magic Angle Spinning (MAS) spectra of ^{11}B and ^{71}Ga nuclei in $GaBO_3$ crystals. A special computer simulation code has been put forward in order to test

* Corresponding author

different JDDs. Indeed, the available NMR simulation programs, e.g., GAMMA, SIMPSON, Winfit, STARS, Wsolids, QUASAR, QuadFit and DMFit, either do not at all take into account the distributions of the NMR parameters or, at best, allow calculations only with "standard" JDDs (e.g. Gauss in DMfit and QuadFit or Czjzek's in QuadFit) [15 23].

2. Comparative analysis of Czjzek's and Maurer's models

2.1. General characteristics

The EFG is described by a second rank tensor $\boldsymbol{V}$ with principal components V_x, V_y and V_z subjected to the restriction that $V_x + V_y + V_z = 0$ [1]. In choosing the principal axes of $\boldsymbol{V}$, the convention $|V_z| \geqslant |V_y| \geqslant |V_x|$ is usually applied. The "asymmetry parameter" η is defined as [1].

$$\eta = \frac{V_x - V_y}{V_z}, \tag{1}$$

so that η remains confined within the range $0 \leqslant \eta \leqslant 1$. For $\eta = 0$, i.e. $V_x = V_y$, one deals with axial distortion, while for $\eta = 1$, i.e. $V_x = 0$ and $V_y = -V_z$, the *absolute* deviation from cubic symmetry is the same along two principal axes of $\boldsymbol{V}$ (the maximum rhombic distortion).

In a disordered solid, all components of $\boldsymbol{V}$ are expected to be statistically distributed. In order to satisfy the requirements of diagonal symmetry and tracelessness, as well as of rotational invariance of $\boldsymbol{V}$, these components are calculated as linear combinations of five normally distributed random quantities U_i, $i = 1, \ldots, 5$, with zero mean values and equal standard deviations $\frac{1}{2}\sigma$ [7,9,24]. (Here the $\frac{1}{2}$ factor has been introduced in order that the subsequent formulae could be expressed in their habitual form [7 9,13,24].) Thus, we get:

$$\boldsymbol{V} = \sqrt{3}\begin{pmatrix} -\frac{1}{\sqrt{3}}U_1 + U_5 & U_4 & U_2 \\ U_4 & -\frac{1}{\sqrt{3}}U_1 - U_5 & U_3 \\ U_2 & U_3 & \frac{2}{\sqrt{3}}U_1 \end{pmatrix}. \tag{2}$$

Note that with this definition σ represents the standard deviation of V_{zz}.

With these assumptions, the Czjzek's JDD takes the form [7,9]:

$$P(V_z, \eta) = \frac{1}{\sqrt{2\pi}}\frac{V_z^4}{\sigma^5}\eta(1 - \tfrac{1}{9}\eta^2)e^{-\frac{1}{2}\frac{V_z^2}{\sigma^2}\left(1+\frac{1}{3}\eta^2\right)} \tag{3}$$

with marginal distributions, respectively, for $-\infty < V_z < \infty$ and $0 \leqslant \eta \leqslant 1$:

$$P_m(V_z) = \sqrt{\frac{2}{\pi}}\frac{1}{\sigma}\left[\left(\frac{3}{2}\frac{V_z^2}{\sigma^2} - 1\right)e^{-\frac{1}{2}\frac{V_z^2}{\sigma^2}} - \left(\frac{4}{3}\frac{V_z^2}{\sigma^2} - 1\right)e^{-\frac{2}{3}\frac{V_z^2}{\sigma^2}}\right]; \; P_m(\eta) = 3\eta\frac{1 - \frac{1}{9}\eta^2}{(1 + \frac{1}{3}\eta^2)^{5/2}}. \tag{4}$$

Alternatively, instead of V_z and η the following parameters can be introduced [8]:

$$\Delta = |V_z|\sqrt{1 + \tfrac{1}{3}\eta^2} \tag{5}$$

and

$$\psi = \begin{cases} \frac{1}{6}\pi - \arctan\frac{1}{\sqrt{3}}\eta & \text{for} \quad V_z > 0 \\ -\frac{1}{6}\pi + \arctan\frac{1}{\sqrt{3}}\eta & \text{for} \quad V_z < 0 \end{cases}. \tag{6}$$

The advantage of the latter representation is that, as a difference of the former one it assures the continuity of the region of non zero probability density of distributed quadrupole parameters, cf. Figs. 1 and 3 in the Czjzek's paper [8]. One can see that $\Delta \geqslant 0$ and $-\frac{\pi}{6} \leqslant \psi \leqslant \frac{\pi}{6}$, $\psi = \pm\frac{\pi}{6}$ and $\psi = 0$ corresponding, respectively, to $\eta = 0$ (axial distor tion) and $\eta = 1$ (maximum rhombic distortion).

For the corresponding form of the Czjzek's JDD one gets [8]:

$$P(\Delta, \psi) = \frac{1}{\sqrt{2\pi}}\frac{\Delta^4}{\sigma^5}\cos 3\psi e^{-\frac{1}{2}\frac{\Delta^2}{\sigma^2}}, \tag{7}$$

and the marginal distributions, for $0 \leqslant \Delta < \infty$ and $-\frac{\pi}{6} \leqslant \psi \leqslant \frac{\pi}{6}$, respec tively, are:

$$P_m(\Delta) = \frac{1}{3}\sqrt{\frac{2}{\pi}}\frac{\Delta^4}{\sigma^5}e^{-\frac{1}{2}\frac{\Delta^2}{\sigma^2}} \; ; \quad P_m(\psi) = \frac{3}{2}\cos 3\psi. \tag{8}$$

In the Maurer's and Le Caër's *et al.* approach [9,13,24], the EFG tensor is represented as a sum of two tensors, $\boldsymbol{V}_0 + \boldsymbol{V}$ where $\boldsymbol{V}$ is the random tensor defined above, and $\boldsymbol{V}_0$ is a fixed traceless tensor describing a "perfect crystal" and characterized by parameters V_{z0} and η_0. In the coordinate frame where $\boldsymbol{V}_0$ is diagonal,

$$\boldsymbol{V}_0 = V_{z0}\begin{pmatrix} \frac{1}{2}(\eta_0 - 1) & 0 & 0 \\ 0 & -\frac{1}{2}(\eta_0 + 1) & 0 \\ 0 & 0 & 1 \end{pmatrix} \tag{9}$$

where

$$\eta_0 = \frac{V_{x0} - V_{y0}}{V_{z0}}. \tag{10}$$

The parameters Δ_0 and ψ_0 are introduced by means of Eqs. (5) and (6), respectively, replacing in the latter V_z by V_{z0} and η by η_0.

(Note that in the Maurer's approach all components of the $\boldsymbol{V}$ tensor are assumed to be normally distributed with zero mean values and equal standard deviations [13]. However, such an assumption does not satisfy the above mentioned requirements for this tensor.)

We have put forward a simulation code implementing the above model.[1] This code

i. generates the normal random quantities U_i, $i = 1, \ldots, 5$, *vide supra*;

i. using Eqs. (2) and (9) computes and diagonalizes the $\boldsymbol{V}_0 + \boldsymbol{V}$ tensor;
ii. for each set of main values of the latter calculates Δ and ψ, respecting the above mentioned convention $|V_z| \geqslant |V_y| \geqslant |V_x|$ and using Eqs. (1), (5) and (6);
iii. builds marginal distribution densities of Δ and ψ as well as the JDD $P(\Delta, \psi)$ for the $\boldsymbol{V}_0 + \boldsymbol{V}$ tensor;
iv. computes mean values $\langle\Delta\rangle$, $\langle\psi\rangle$, standard deviations σ_Δ, σ_ψ and a correlation coefficient ρ of Δ and ψ.

Figs. 1 3 illustrate variations of the latter parameters with σ for different Δ_0 and ψ_0.

The graph of $\langle\Delta\rangle$ vs. σ is shown in Fig. 1 (left). In the case of $\Delta_0 = 0$, corresponding to the Czjzek's JDD (obviously, in this case $\psi_0 = 0$ as well), the increase of $\langle\Delta\rangle$ with the increase of σ is strictly linear; indeed, the marginal distribution $P_m(\Delta)$, see Eq. (8), yields:

$$\langle\Delta\rangle = \frac{16}{3}\sqrt{\frac{2}{\pi}}\sigma \approx 4.2554\sigma. \tag{11}$$

For $\Delta_0 \neq 0$ and different values of ψ_0, $\langle\Delta\rangle$ tends to Δ_0 when σ tends to 0 and asymptotically reaches the trend given by Eq. (11) for $\sigma \gg \Delta_0$. From Fig. 1 (right) one can see that $\langle\psi\rangle$ tends to ψ_0 when σ tends to 0 and tends to zero for $\sigma \gg \Delta_0$. If $\psi_0 = 0$, $\langle\psi\rangle$ is always zero, including the case $\Delta_0 = 0$ corresponding to the Czjzek's JDD.

With an increase of σ, both σ_Δ and σ_ψ increase, see Fig. 2. For $\Delta_0 = 0$ one can readily show that

[1] Available on request from the authors.

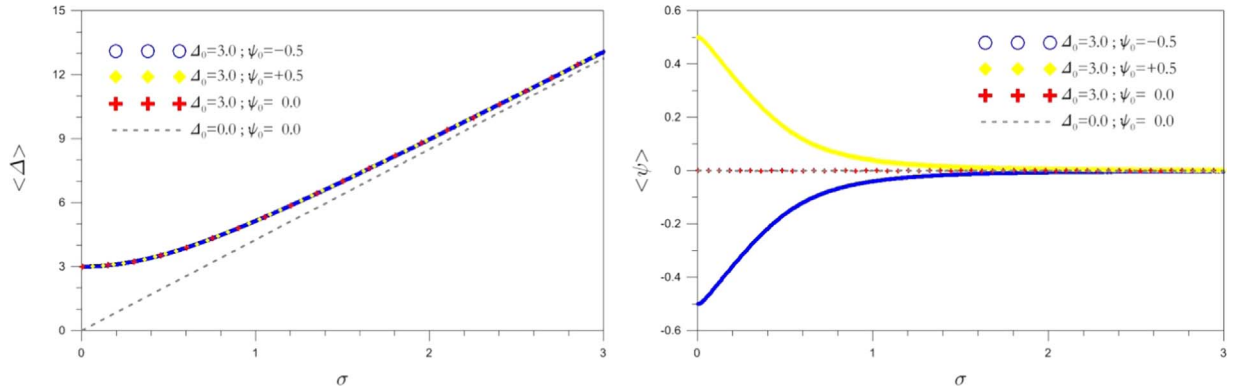

Fig. 1. Dependences on σ of $\langle\Delta\rangle$ (left) and $\langle\psi\rangle$ (right) for different Δ_0 and ψ_0. The dashed line in the left part of the figure corresponds to Eq. (11). Δ_0, σ and $\langle\Delta\rangle$ are in arbitrary units.

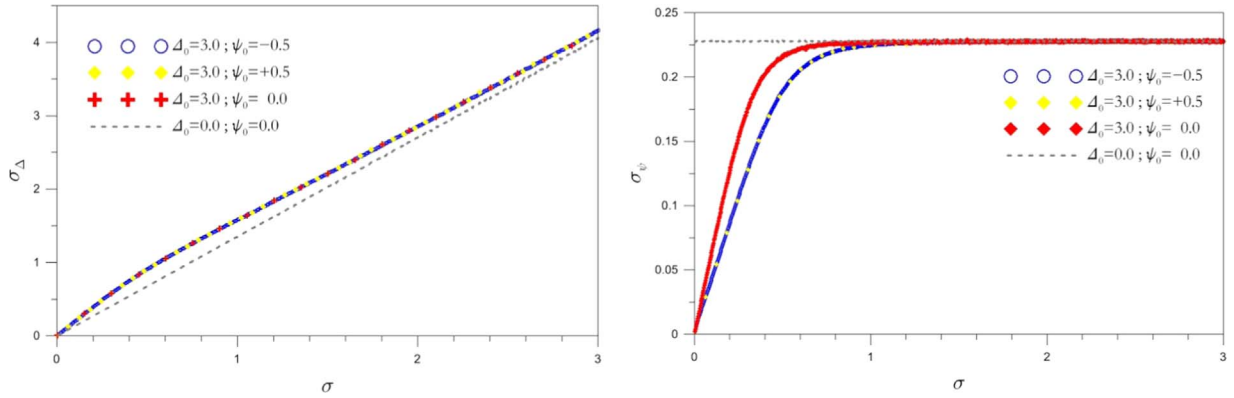

Fig. 2. Dependences on σ of σ_Δ (left) and σ_ψ (right) for different Δ_0 and ψ_0. The dashed lines in the left and right parts correspond to Eqs. (12) and (13), respectively. Δ_0, σ and σ_Δ are in arbitrary units.

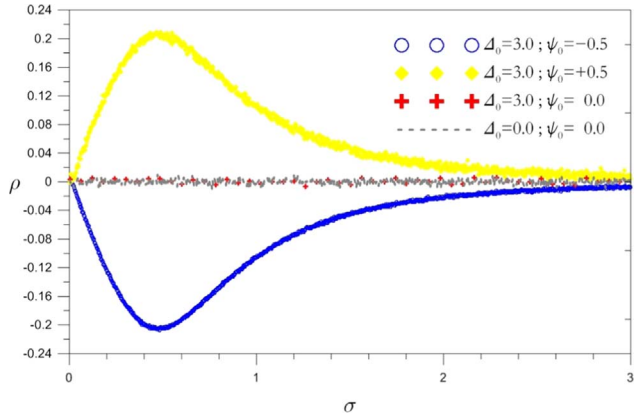

Fig. 3. Relationships between ρ and σ for different Δ_0 (in arbitrary units) and ψ_0.

$$\sigma_\Delta = \frac{2}{3}\sqrt{45 - \frac{128}{\pi}}\,\sigma \approx 1.3754\sigma. \tag{12}$$

For $\Delta_0 \neq 0$ the relationship between σ_Δ and σ becomes non linear, and the trend given by Eq. (12) is reached asymptotically for $\sigma \gg \Delta_0$. In the latter case, as shown in Fig. 2 (right), σ_ψ tends to its limiting value, corresponding to that of the Czjzek's JDD. Using the marginal distribution $P_m(\psi)$, see Eq.(8), one gets:

$$\lim_{\sigma\to\infty}\sigma_\psi = \frac{1}{6}\sqrt{\pi^2 - 8} \approx 0.2279. \tag{13}$$

Fig. 5 in the Maurer's paper [13] suggests that the correlation between Δ and ψ tends to decrease with increasing the departure from axial symmetry (*viz.*, increasing η_0) and with lowering the degree of disorder (*viz.*, increasing the Δ_0/σ ratio). However, Fig. 3 below shows that this is only a part of a more general trend: indeed, ρ vanishes for any degree of disorder if $\psi_0 = 0$ as well as in the limits of both low and high disorder. The absolute value of ρ attains a maximal value of *ca.* 0.21 for $\psi_0 = \pm\frac{\pi}{6}$ (i.e., for axial symmetry) at intermediate degree of disorder. The corresponding value of σ, σ_{max}, is proportional to Δ_0; numerical calculations yield the following relationship between these parameters:

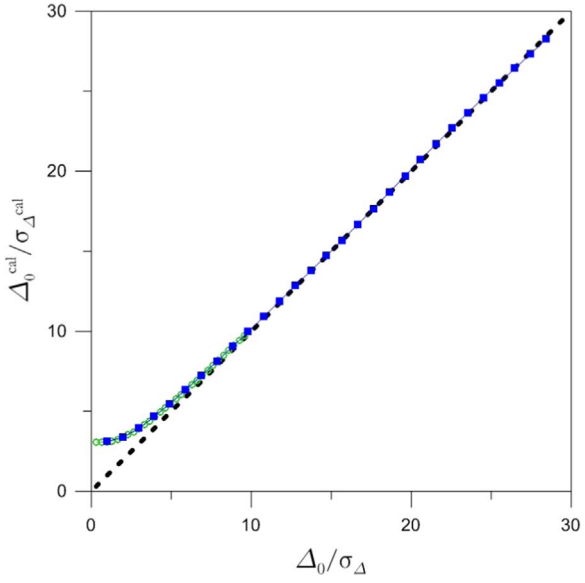

Fig. 4. Relationships between Δ_0/σ_Δ and $\Delta_0^{cal}/\sigma_\Delta^{cal}$ for $\psi_0 = 0.5$: $\sigma_\Delta = 0.102$ a. u., $\sigma_\psi = 0.024$, $\rho = 0.033$ (squares, blue online) and $\sigma_\Delta = 0.303$ a. u., $\sigma_\psi = 0.066$, $\rho = 0.097$ (circles, green online). The dashed line corresponds to $\Delta_0^{cal}/\sigma_\Delta^{cal} = \Delta_0/\sigma_\Delta$. (For interpretation of the references to color in this figure legend, the reader is referred to the web version of this article.)

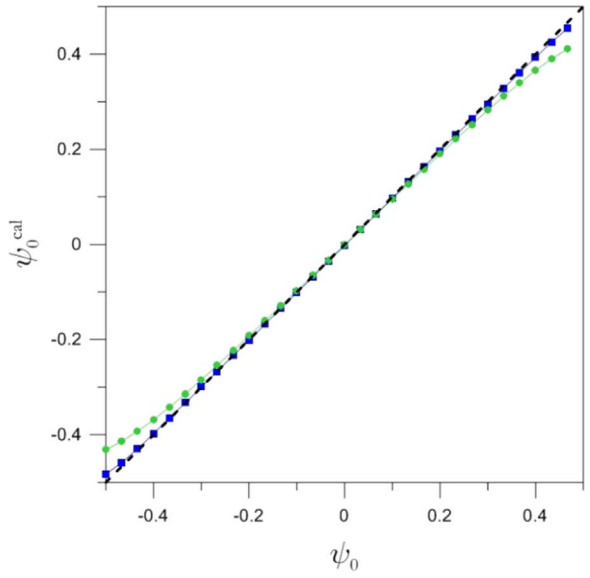

Fig. 5. Relationships between ψ_0 and ψ_0^{cal} for $\Delta_0 = 3.0$ a. u.: $\sigma_\Delta = 0.102$ a. u., $\sigma_\psi = 0.024$, $\rho = 0.033$ (squares, blue online) and $\sigma_\Delta = 0.303$ a. u., $\sigma_\psi = 0.066$, $\rho = 0.097$ (circles, green online). The dashed line corresponds to $\psi_0^{cal} = \psi_0$. (For interpretation of the references to color in this figure legend, the reader is referred to the web version of this article.)

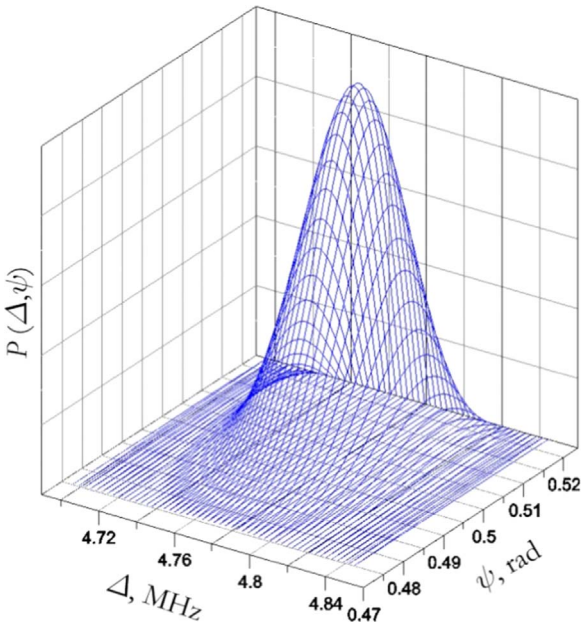

Fig. 7. Maurer's JDD calculated with the parameters of the computer-generated spectrum shown in Fig. 6 for ^{71}Ga. The JDD for ^{11}B has a qualitatively similar shape.

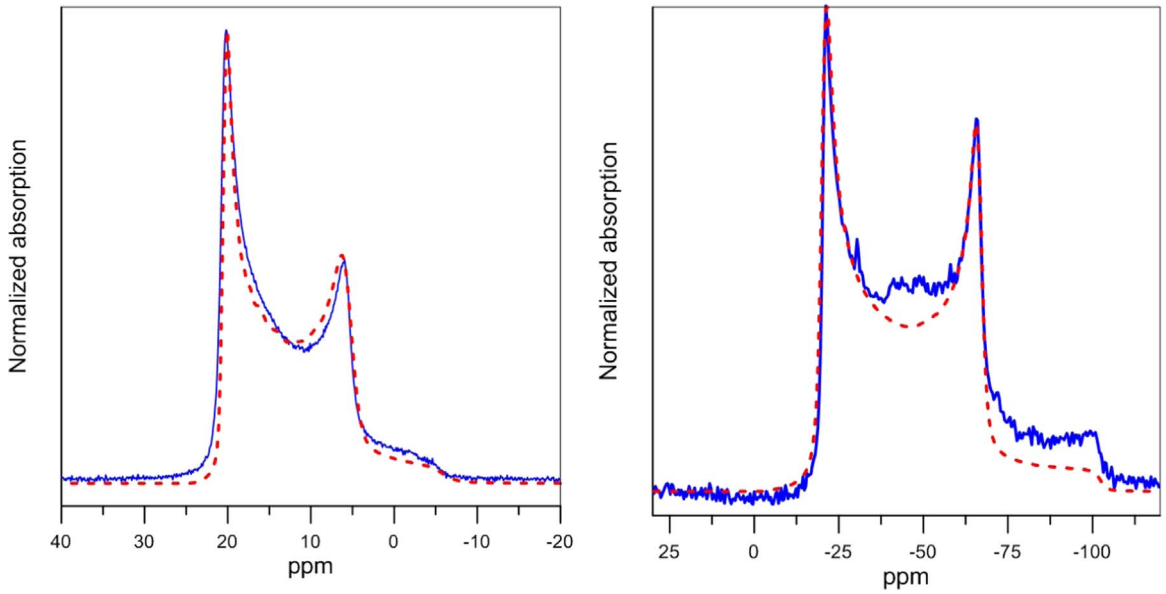

Fig. 6. Experimental MAS NMR spectra (solid, blue online) for ^{11}B (left) and ^{71}Ga (right) and the corresponding best-fit computer-generated spectra using the Maurer's JDD (dashed, red online). The simulation parameters are: for ^{11}B, $\delta_{iso} = 24.7$ppm, $\Delta_0 = 2.84$MHz, $\sigma_\Delta = 0.04$MHz, $\psi_0 = \frac{\pi}{6}$, $\sigma_\psi = 0.011$ and $\rho = 0.1$ [25], and for ^{71}Ga, $\delta_{iso} = -6.9$ ppm, $\sigma_\delta = 0.4$ ppm, $\Delta_0 = 4.77$ MHz, $\sigma_\Delta = 0.02$ MHz, $\psi_0 = 0.523$, $\sigma_\psi = 0.013$ and $\rho = 0.0$. (For interpretation of the references to color in this figure legend, the reader is referred to the web version of this article.)

$$\sigma_{max} \approx 0.16\Delta_0 . \tag{14}$$

2.2. Analytical Maurer's JDD

Besides, Maurer [13] has introduced an empirical analytical JDD by associating the marginal distribution of $\delta = \Delta/\sigma$, derived from a non central χ^2 distribution with five degrees of freedom, with a semi heuristic marginal distribution of ψ and allowing for a certain correla tion between both random variables.

Here we prefer using σ_Δ instead of σ; indeed, such a choice seems more appropriate for a bivariate JDD $P(\Delta, \psi)$. After amending for a clerical error (in the third term inside the brackets of the exponent in Eq. (10) of the Maurer's paper [13], ρ should be replaced by -2ρ), this JDD becomes:

$$P(\Delta, \psi) \propto \frac{\Delta}{\sigma_\Delta} g(x) \cos 3\psi \; e^{-\frac{1}{2}\frac{1}{1-\rho 2}\left[\frac{(\Delta-\Delta_0)^2}{{\sigma_\Delta}^2}+\frac{(\psi-\psi_0)^2}{{\sigma_\psi}^2}-2\rho\frac{(\Delta-\Delta_0)(\psi-\psi_0)}{\sigma_\Delta\sigma_\psi}\right]} \tag{15}$$

where

$$g(x) = x - 1 + (x+1)e^{-2x} \;\text{ and }\; x = \frac{\Delta\Delta_0}{{\sigma_\Delta}^2}. \tag{16}$$

Of course, the use of an analytical JDD considerably simplifies the analysis of the experimental results; yet, the limits of its applicability should be carefully evaluated. With this aim in view, we have examined the relations between the "input" parameters Δ_0, ψ_0, ρ and σ_Δ occur ring in Eq. (15) and the corresponding "output" parameters

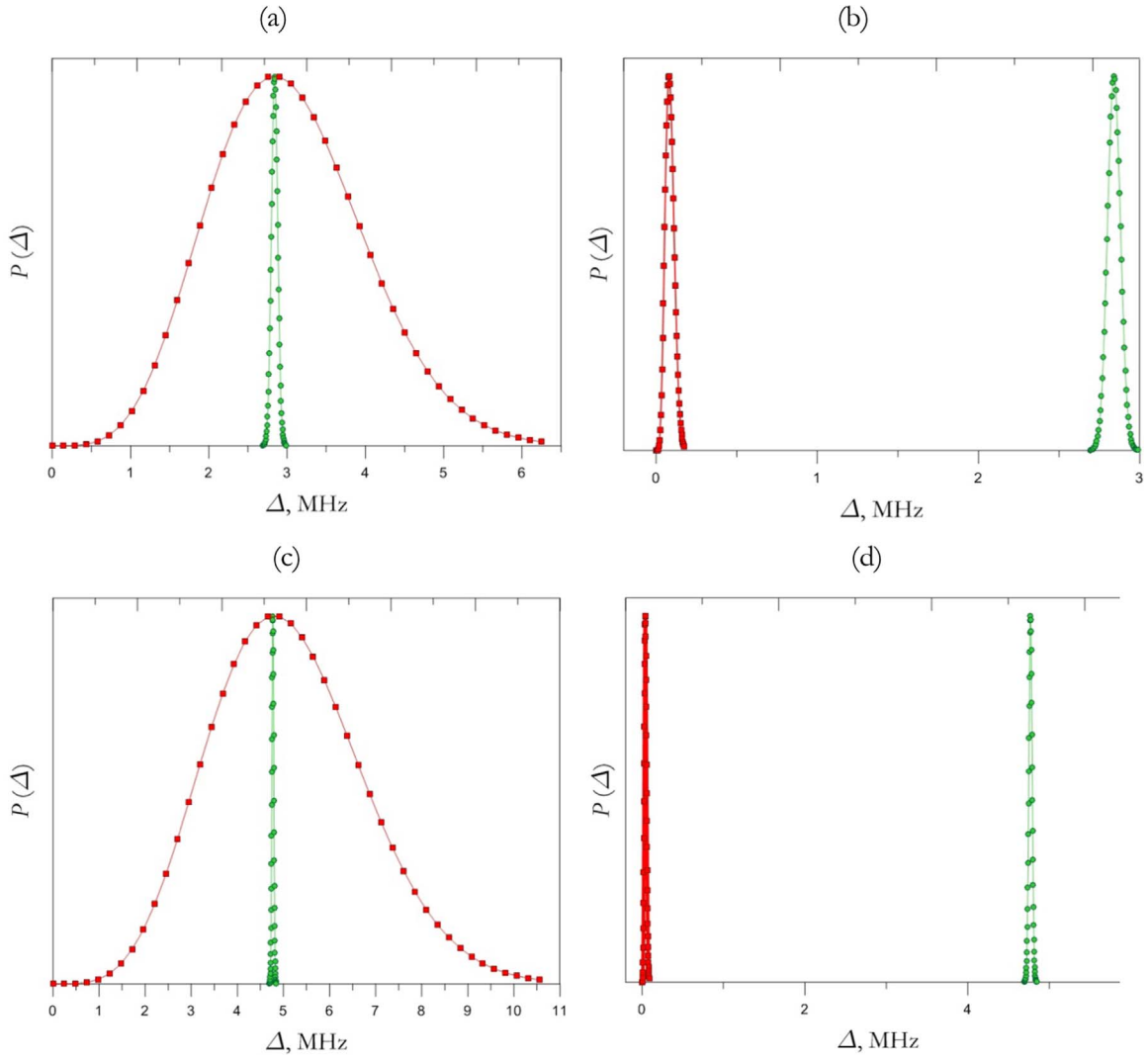

Fig. 8. Marginal distributions of Δ for ^{11}B (a and b) and ^{71}Ga (c and d) obtained for the Maurer's (points, green online) and Czjzek's (squares, red online) models. The parameters of the Maurer's distribution correspond to the best-fit shown in Fig. 6. For the Czjzek's distribution, for ^{11}B $\sigma = 1.42$ (a) and $\sigma = 0.04$MHz (b), and for ^{71}Ga $\sigma = 2.4$ (c) and $\sigma = 0.02$MHz(d). (For interpretation of the references to color in this figure legend, the reader is referred to the web version of this article.)

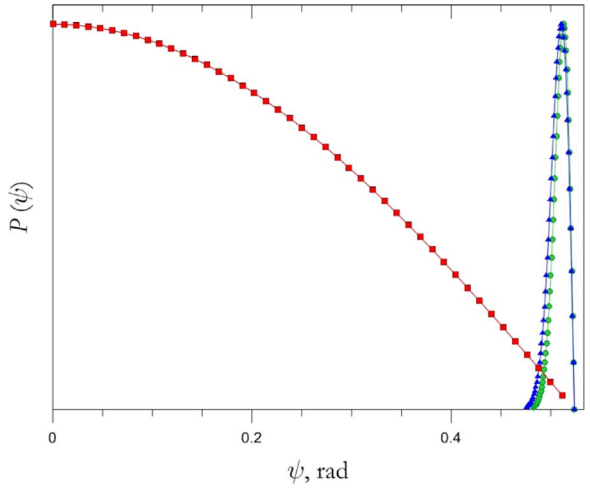

Fig. 9. Marginal distributions of ψ obtained for the Maurer's for ^{11}B (points, green online) and ^{71}Ga (triangles, blue online) and Czjzek's (squares, red online) models. The parameters of the Maurer's distribution correspond to the best-fits shown in Fig. 6. (For interpretation of the references to color in this figure legend, the reader is referred to the web version of this article.)

Δ_0^{cal}, ψ_0^{cal}, ρ^{cal} and σ_Δ^{cal}, i.e., the characteristics of the JDD $P(\Delta, \psi)$, calculated for different Δ_0/σ_Δ ratios. As far as σ and σ_ψ are interrelated, the values of the latter parameter have been chosen in accordance with the relationships shown in Fig. 2. The values of ρ have been chosen from the data displayed in Fig. 3.

Figs. 4 and 5 show the results of this analysis. In both figures Δ_0, Δ_0^{cal} and σ_Δ are expressed in arbitrary units (a. u.). In Fig. 5 the data are presented for two cases: $\Delta_0/\sigma_\Delta \approx 30$ (squares, blue online) and $\Delta_0/\sigma_\Delta \approx 10$ (circles, green online).

As one can see, for relatively low disorder, $\Delta_0/\sigma_\Delta \approx 30$, the "input" and "output" parameters are in good agreement; however, at higher disorder, e.g., already at $\Delta_0/\sigma_\Delta \approx 10$, these parameters considerably differ from each other. In Figs. 4 and 5 we show the results only for $\psi_0 = 0.5$, as far as in the low disorder case those for $\psi_0 = 0$ and $\psi_0 = -0.5$ are almost the same. For higher disorder, the results for $\psi_0 = \pm 0.5$ are still very close to each other. For $\psi_0 = 0$ the discrepancy between the "input" and "output" parameters becomes more pro nounced, but in any case we are outside the limits of applicability of the analytical Maurer's JDD.

3. Experimental results and discussion

^{11}B and ^{71}Ga MAS NMR spectra of $GaBO_3$, ground to powder were

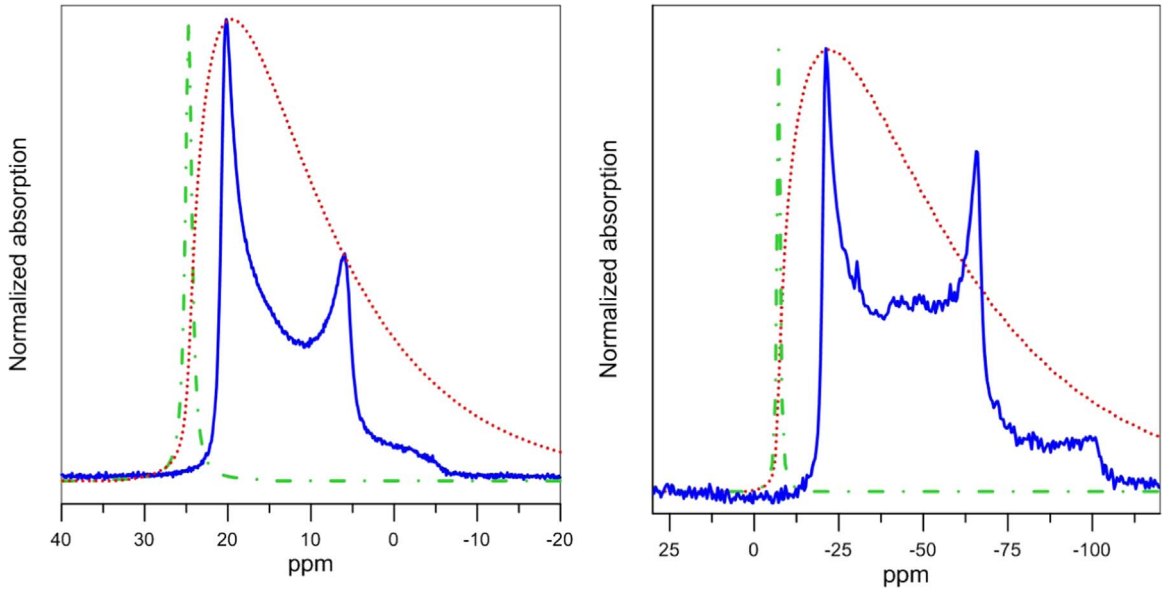

Fig. 10. Experimental (solid, blue online) for ^{11}B (left) and ^{71}Ga (right) and corresponding computer-generated NMR spectra for the Czjzek's JDD. The simulation parameters are: for ^{11}B, $\sigma = 1.42$ (dotted, red online) and $\sigma = 0.04$ MHz (dashed-dotted, green online), and for ^{71}Ga, $\sigma = 2.4$ (dotted, red online) and $\sigma = 0.02$ MHz (dashed-dotted, green online). (For interpretation of the references to color in this figure legend, the reader is referred to the web version of this article.)

measured with a Bruker Avance 400 NMR spectrometer. The measure ments of ^{11}B spectra have been described in our previous paper [25]. The measurements of ^{71}Ga spectra have been carried out at the corresponding resonance frequency, 122.0564 MHz, with 4 mm rotors at the spinning rate of 14 kHz. The absorption signal was recorded using classical direct acquisition by single pulse free induction decay (FID) excitation with accumulation of 1000 pulse signals repeated with 2.4 μs radiofrequency pulse length. The NMR spectra were obtained by a Fourier transform of the FID signals.

The ^{11}B and ^{71}Ga NMR spectra were computer simulated using laboratory developed codes. Computer generated spectra have been acquired by integrating over distributed values of the spin Hamiltonian parameters and random orientations of crystallites.

Fig. 6 shows the experimental spectra for ^{11}B (left) [25] and ^{71}Ga (right) together with corresponding best fit computer generated spec tra for the Maurer's JDD. The simulation procedure for ^{71}Ga spectra has been similar to that for ^{11}B [25]; however, in order to obtain closer fittings, a normal distribution of δ_{iso} with a standard deviation σ_δ has also been assumed.

One can see that the Maurer's JDD provides satisfactory fits to the experimental MAS NMR spectra using fairly reasonable parameter values. The remaining discrepancy between the computer generated and experimental spectra for ^{71}Ga can be caused by an ill resolved superimposed resonance, probably arising from ^{71}Ga nuclei in more disordered environment and/or by a superposed contribution from non central NMR transitions.

The best fit simulation parameters for ^{71}Ga NMR spectra are consistent with sixfold coordinated gallium sites [26]. $FeBO_3$ crystals have calcite structure where each iron is surrounded by six oxygens forming a nearly perfect octahedron [27]. As far as $Fe_xGa_{1-x}BO_3$ are isomorphous to $FeBO_3$ [28], it can be reasonably assumed that Ga ions are also sixfold coordinated, and this is confirmed by the NMR results.

One might wonder if adequate fitting to the above experimental spectra can be achieved with the Czjzek's JDD. Obviously, in this case one should be able by varying the only adjustable parameter σ to simultaneously obtain in the simulations the mean parameter values $\langle\Delta\rangle$ and $\langle\psi\rangle$ close, respectively, to Δ_0 and ψ_0 obtained with the Maurer's JDD and similar distribution widths of these parameters.

Fig. 7 shows the three dimensional JDD for the Maurer's model, and Figs. 8 and 9 show the corresponding marginal distributions of Δ and ψ. In the latter two figures we have also shown for the Czjzek's model the marginal distributions of Δ and ψ yielding the required mean values of these parameters for the Maurer's model. One can see that in order to obtain $\langle\Delta\rangle$ values close to Δ_0 we need very high σ values, resp., unrealistically broad distributions of Δ, cf. Fig. 8 (a and c). On the other hand, taking the same distribution widths of Δ as those determined with the Maurer's JDD (σ_Δ), in the case of the Czjzek's JDD would result in very low mean Δ values, 0.08 and 0.04 MHz for ^{11}B and ^{71}Ga, respectively, cf. Fig. 8 (b and d).

Moreover, the Czjzek's JDD, as expected from Eq. (8), regardless of the σ value, always gives one and the same, extremely broad marginal distribution of ψ, see Fig. 9. Obviously, such a distribution is incompatible with only slightly perturbed axial site symmetry in the crystal. In contrast, the Maurer's JDD can produce quite narrow marginal distributions of ψ, describing weak random distortions from the perfect structure.

Fig. 10 compares the experimental NMR spectra for ^{11}B and ^{71}Ga with computer generated spectra using the Czjzek's JDD with the same σ values as in Fig. 8. Obviously, in contrast to the Maurer's model, the Czjzek's model flagrantly fails to describe the experimental results. This result is not surprising; indeed, as we have seen above, the Czjzek's JDD, in principle, contains no information on the crystal structure. In contrast, the Maurer's JDD includes mean values Δ_0, ψ_0 and separate distribution widths of both random variables Δ and ψ, as well the correlation coefficient ρ between them, thus preserving to a certain extent the information on intrinsic symmetry and ordering in crystals with low local disorder.

4. Conclusions

We have carried out comparative analysis of Czjzek's and Maurer's models of the JDD of the NMR quadrupole parameters. In the case of the Maurer's model, we have considered both the numerical and the analytical JDD of the random parameters Δ and ψ, and we have put forward a computer code allowing to obtain the dependences of the corresponding mean values $\langle\Delta\rangle$, $\langle\psi\rangle$, standard deviations σ_Δ, σ_ψ and correlation coefficient ρ on the input value of σ, proportional to the degree of local disorder. The obtained relationships have allowed to determine the limits of applicability of the analytical Maurer's JDD.

The Czjzek's JDD is relatively well adapted to the case of heavily

disordered solids; meanwhile it contains only one adjustable parameter, describing the degree of local disorder and does not include the characteristics of local structure, partially preserved in the presence of a low degree of disorder. As a result, the marginal distribution of the parameter ψ, describing the local symmetry, becomes extremely broad, which is incompatible with the existence of short range ordering. In contrast, the Maurer's JDD has no these drawbacks, therefore it is expected to provide satisfactory fits to experimental NMR spectra in crystals with low local disorder.

The above considerations have been corroborated by applying the Czjzek's and Maurer's models to computer simulations of MAS NMR spectra of ^{11}B and ^{71}Ga isotopes in gallium borate. With the former distribution no adequate description can be obtained while the latter has provided quite satisfactory fits.

The present study shows that the Czjzek's model should not be used in computer assisted analysis of NMR spectra of materials with low degree of local disorder. On the other hand, the Maurer's model, conceptually well adapted to this situation, can provide quite satisfactory fits to the experimental NMR spectra.

Acknowledgements

This work was partially supported by the Russian Foundation for Basic Research and the Ministry of Education, Science and Youth of the Republic of Crimea, in the framework of scientific project Grant No. 15 42 01008 “р юг а”.

References

[1] A. Abragam, The Principles of Nuclear Magnetism, Clarendon, Oxford, 1961.
[2] D. Freude, Quadrupolar Nuclei in Solid-State Nuclear Magnetic Resonance, in Encyclopedia of Analytical Chemistry, R.A. Meyers (Ed.), p. 12188, 2000.
[3] K. Seleznyova, M. Strugatsky, S. Yagupov, N. Postivey, A. Artemenko, J. Kliava, Phys. Status Solidi B 251 (2014) 1393.
[4] J. Kliava, Phys. Status Solidi B 134 (1986) 411.
[5] J.-B. d’Espinose de Lacaillerie, C. Fretigny, D. Massiot, J. Magn. Reson. 192 (2008) 244.
[6] A. Bals, S.I. Gorbachuk, J. Kliava, N.G. Kakazei, Phys. Status Solidi A 114 (1989) 305.
[7] G. Czjzek, J. Fink, F. Gotz, H. Schmidt, J.M.D. Coey, J.P. Rebouillat, A. Lienard, Phys. Rev. B: Condens. Matter 23 (1981) 2513.
[8] G. Czjzek, Hyperfine Interact. 14 (1983) 189.
[9] G. Le Caër, R.A. Brand, J. Phys.: Condens. Matter 10 (1998) 10715.
[10] J. Kliava, R. Berger, Y. Servant, J. Emery, J.-M. Greneche, J. Trokšs, J. Non-Cryst. Solids 202 (1996) 205.
[11] C. Legein, J.-Y. Buzaré, G. Silly, C. Jacoboni, J. Phys.: Condens. Matter 8 (1996) 4339.
[12] C. Legein, J.-Y. Buzaré, J. Emery, C. Jacoboni, J. Phys.: Condens. Matter 7 (1995) 3853.
[13] M. Maurer, Phys. Rev. B 34 (1986) 8996.
[14] J. Kliava, R. Berger, J. Magn. Magn. Mater. 205 (1999) 328.
[15] S.A. Smith, T.O. Levante, B.H. Meier, R.R. Ernst, J. Magn. Res. Ser. A 106 (1994) 75.
[16] M. Bak, T. Rasmussen, N.C. Nielsen, J. Magn. Res. 147 (2000) 296.
[17] D. Massiot, H. Thiele, A. Germanus, WinFit, Bruker Report, 140 43, 1994.
[18] Henrik Bildsøe, STARS Package, Aarhus University, Denmark, Varian: Palo Alto, CA.
[19] K. Eichele, R.E. Wasylishen, Wsolids NMR Simulation Package ⟨http://anorganik.uni-tuebingen.de/klaus/soft/⟩, 2001.
[20] J.P. Amoureux, C. Fernandez, P. Granger, NATO ASI Ser. C322 (1990) 409.
[21] J.P.. Amoureux, C.. Fernandez, QUASAR Solid-State NMR Simulation for Quadrupolar Nuclei, Université de Lille, France.
[22] T.F. Kemp, M.E. Smith, Solid State NMR 35 (2009) 243.
[23] D. Massiot, F. Fayon, M. Capron, I. King, S. Le Calve, B. Alonso, J.-O. Durand, B. Bujoli, Z. Gan, G. Hoatson, Magn. Res. Chem. 40 (2002) 70.
[24] G. Le Caër, B. Bureau, D. Massiot, J. Phys.: Condens. Matter 22 (2010) 065402.
[25] K. Seleznyova, N. Sergeev, M. Olszewski, P. Stępień, S. Yagupov, M. Strugatsky, J. Kliava, Solid State Nucl. Magn. Reson. 70 (2015) 38.
[26] D. Massiot, T. Vosegaard, N. Magneron, D. Trumeau, V. Montouillout, P. Berthet, T. Loiseau, B. Bujoliet, Solid State NMR 15 (1999) 159.
[27] R. Diehl, W. Jantz, B.I. Nolang, W. Wettling, in: Current Topics in Materials Science, E. Kaldis ed., Elsevier, New-York, V. 11 (1984) 241.
[28] S. Yagupov, M. Strugatsky, K. Seleznyova, E. Maksimova, I. Nauhatsky, V. Yagupov, E. Milyukova, J. Kliava, Appl. Phys. A 121 (2015) 179.